Journal of Solid State Chemistry **156,** 57–60 (2001)
doi:10.1006/jssc.2000.8958, available online at http://www.idealibrary.com on IDEAL®

Comparison of Electrical Properties between Fluoroapatite and Hydroxyapatite Materials

A. Laghzizil,*,[1] N. El Herch,* A. Bouhaouss,* G. Lorente,† and J. Macquete†

*Laboratoire de Chimie Physique Générale, Dépatement de Chimie, Faculte des Sciences, Universite Mohamed V—Agdal, BP 1014, Rabat, Morocco; and †Laboratoire de Chimie de la Matière Condensée, Université Pierre et Marie Curie, 4 place Jussieu, 75252 Paris, France
E-mail: laghzizi@fsr.ac.ma

Submitted June 14, 2000; in revised form August 14, 2000; accepted September 5, 2000; published online January 3, 2001

By appropriate modifications of existing precipitation methods, apatite samples of formula $M_{10}(PO_4)_6X_2$ (M = Ca, Pb, Ba and X = F, OH) were prepared at 80°C. Samples were characterized using X-ray diffraction, infrared, ^{31}P NMR, SEM, and chemical analysis. By comparing the effect of fluoride and hydroxide ions on ionic conductivity measurements, it was concluded that the fluorinated materials (MFAp) were better conductors than other hydroxyapatites (MHAp). The F^- and H^+ ions are the main charge carriers, respectively, in fluoroapatite and in hydroxyapatite compounds. The most pronounced effect on the conduction properties was observed in the lead apatite material. These results should provide important physico-chemical information for ionic diffusion of the roles played by fluoride in inhibiting dental caries. © 2001 Academic Press

Key Words: **Apatites; substitutions; complex impedance; mobility; ionic conductivity.**

1. INTRODUCTION

Fluoro- and hydroxyapatites with a crystallographical analogue to calcified tissues of vertebrates are largely studied in relation with their physico-chemical properties (1–5). The important characteristics of these materials are related to their structure, which belongs to the hexagonal (space group $P6_3/m$). The large tunnels along the c axis induce a good diffusion of anionic species (X^-). Gas sensor (6) and catalytic property (7) can be in relation with electrical properties of apatite materials. Recently, we have established a correlation between electrical and structural properties of unsubstituted and substituted fluoroapatites (8–10). The present study is devoted to the electrical behavior of hydroxyapatite and fluoroapatite materials $M_{10}(PO_4)_6X_2$ (where M = Ca, Pb, Ba and X = F, OH) using a complex impedance method in order to master the effects of M^{2+} cations on the ionic conductivity (F^- and H^+ ions). For this reason, cationic exchange in hydroxyapatite and in fluoroapatite structure is realized. A comparison of ionic conductivity between the fluoroapatites and hydroxyapatites is discussed.

[1] To whom correspondence should be addressed.

2. EXPERIMENTAL

Powdered samples were prepared by precipitation from aqueous solutions with mixing stoichiometric amounts of aqueous solutions of $(NH_4)_2HPO_4$, $Ca(NO_3)_2$, $4H_2O$, $Ba(NO_3)_2$, $Pb(NO_3)_2$, and NH_4F (Merck, 99%). The pH of the solution must be maintained above 10 via the addition of ammonia concentrate (25%). The temperature of the reaction was around 80°C. The barium hydroxyaptite was prepared by the neutralization method using $Ba(OH)_2$ and phosphoric acid at room temperature.

X-ray diffractograms were collected with a Philips PW131 diffractometer using a Cu anticathode. From X-ray diffraction data, the lattice parameters a and c were found using the least-squares method (affpar program). Infrared spectra were recorded on a Perkin–Elmer 457 spectrophotometer using KBr pellets. NMR spectra were recorded on a Bruker MSL 300 spectrometer equipped with an Andrew-type rotor rotating at the frequency of approximately 10 kHz. Experiments were performed at room temperature.

Electrical conductivity measurements of apatite materials were undertaken using the impedance method on a HP4192A impedance meter between 200 and 800°C with the signal frequency ranging from 5 Hz to 13 MHz. Powders were pressed under 5 tons/cm^2 and sintered at 1200°C for Ca, Ba apatites and at 1000°C for Pb apatite. Their compactness was around 85–90% for all samples. Electrodes were prepared by painting Pt paste on both sides of the sintered pellet surfaces, which were then heated at 600°C to ensure a good electrical contact.

0022-4596/01 $35.00
Copyright © 2001 by Academic Press
All rights of reproduction in any form reserved.

3. RESULTS AND DISCUSSIONS

3.1. Characterization

X-ray patterns of the samples reveal the existence of a single phase and are indexed on the basis of the hexagonal system (space group $P6_3/m$). Table 1 shows the lattice parameters a and c for the apatite samples. When Ca^{2+} ions are replaced by Pb^{2+} or Ba^{2+} ions, an increase of a and c suggests a dilatation of the unit cell, which relates to the ionic radius of an M^{2+} ion. When the a and c values of the fluoroapatite and hydroxyapatite samples are compared, the change is due to the ionic radius of OH^-, which is superior than the F^- species. Since all apatites are similar in crystal structure, it is interesting to note that the relative low crystallinity, when F^- is completely replaced by OH^- ions, is due to the disorder of the crystal. This has been confirmed by scanning electronic microscopy, which found particular differences in morphology and size of the individual crystals.

Table 2 shows the infrared spectral assignments for the fluoroapatite and hydroxyapatite samples. When the Ca^{2+} ions are replaced by Pb^{2+} or Ba^{2+} ions, the PO_4 bands shift due to the difference of electronic density on the P–O bond (force constant) and to the M^{2+} size. However, the stretching frequency of the OH bands observed in the hydroxyapatite samples depends on the relative geometry of the OH^- as indicated in several works (11, 12).

For all apatite powders, ^{31}P NMR spectra only show a single signal (versus H_3PO_4). This confirms that one crystallographic site is available for PO_4 tetrahedral independent of the susbtitution of Ca^{2+} ions for larger cations such as Pb^{2+} or Ba^{2+} ions. For example, in hydroxyapatites, the low displacement of chemical shift when Ca^{2+} ions (2.87 ppm) are replaced by Ba^{2+} (1.20 ppm) or Pb^{2+} (0.18 ppm) ions is due to the cation size. These results are in good agreement with those observed in infrared and X-ray diffraction.

Based on the chemical analysis, the amount of metal (M), phosphorus (P), and fluorine (F) found resulted in an M/P ratio (metal/phosphorus) of 1.67 and % F = 3.7%, which are in agreement with the stoichiometric values. This justifies the purity of samples and the suitability of the method adopted for synthesis with the operator conditions used as well as for chemical analysis.

TABLE 1
Lattice Constants a and c for Synthetic Apatites

		M^{2+}		
X^-		Ca^{2+}	Pb^{2+}	Ba^{2+}
F^-	(a, ± 0.003) Å	9.375	9.755	10.104
	(c, ± 0.003) Å	6.875	7.245	7.695
OH^-	(a, ± 0.003) Å	9.432	9.905	10.192
	(c, ± 0.003) Å	6.883	7.201	7.701

TABLE 2
Frequencies (in cm^{-1}) and Assignments of the Bands in Infrared Spectra of MXAp (M = Ca, Pb, Ba and X = F, OH)

Vibration mode	CaHAp	CaFAp	PbHAp	PbFAp	BaHAp	BaFAp
ν_s(OH)	3520	—	3559	—	3606	—
ν_l(OH)	630	—	609	—	620	—
$\nu_3(PO_4)$	1090	1095	1041	1041	1060	1060
	1070	—	985	980	1020	1015
	1040	1045				
$\nu_1(PO_4)$	960	965	930	930	950	937
$\nu_4(PO_4)$	602	600	576	575	586	585
	572	575	550	545	567	562
			540	—	555	—
$\nu_2(PO_4)$	474	475	430	440	460	450
	—	325, 275	415	385	450	385, 300

3.2 Electrical Properties

Complex impedance plots exhibit two semi-circles especially at high temperature. The bulk intrinsic resistance was deduced from the high-frequency intersection of the semi-circle with the real axis. Figures 1 and 2 show the Arrhenius plots of the ionic conductivity, respectively, for the hydroxyapatite and fluoroapatite materials. Table 3 compares the electrical behavior between MFAp and MHAp apatites. It can be observed that the lead apatite (PbFAp and

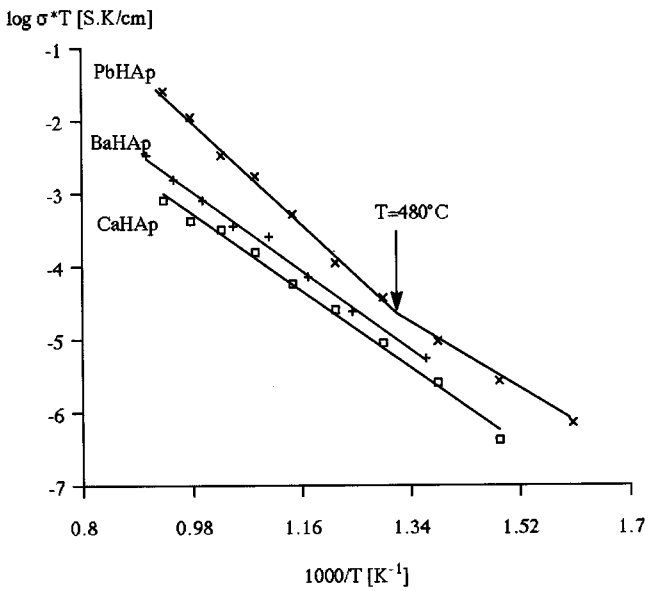

FIG. 1. Arrhenius plots of the ionic conductivity for hydroxyapatite materials MHAp (M = Ca, Pb, Ba).

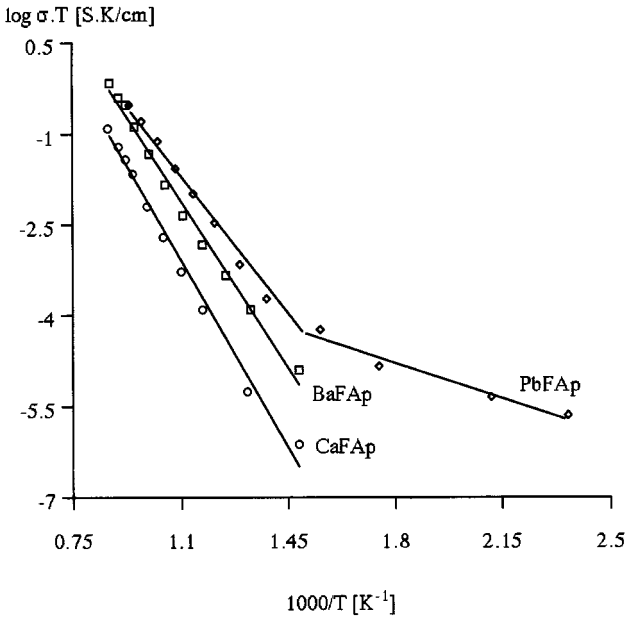

FIG. 2. Arrhenius plots of the conductivity for fluoroapatite materials *M*FAp (*M* = Ca, Pb, Ba).

PbHAp) presents a conductivity higher than that of other apatites. This related particularly to the high polarizability of the Pb^{2+} ion. However, the large tunnels that are a result of introducing large cations such as Ba^{2+} ion can be a second parameter influencing the variation of the ionic conductivity. The break of Arrhenius lines at $T = 480°C$ for the Pb apatite is related to the pseudo-ionic bond Pb–*X* bond, which necessities a high energy to romper this bound and to liberate the mobile ions (F^- or H^+). It is interesting to note also that there is no suggestion of electronic conductivity in this sample, because the polarographic study has been established to confirm this phenomenon. We have indicated no reduction peak of Pb^{4+} ions especially in lead fluorapatite (15).

When compared, the calcium fluoroapatite is a better conductor than the calcium hydroxyapatite material (Fig. 3). Conductivities are essentially due to the hopping ions. In fluoroapatite electrolytes, the conduction mechanism is related to the translational hopping of fluoride ions along the *c* axis of the unit cell from ordinary lattice sites in interstitial sites and back again, which are the only candidates for such a conduction process. The fluoride ions must be able to move to other positions by the formation of thermally actived defects such as Schottky defects with high activation energies, because the fluoroapatite materials are stoichiometric.

In contrast to fluoride conduction, the proton mobility mechanism makes the situation different, calling for a different explanation. Two distinct proton conduction mechanisms can be formulated in hydroxyapatite conductors: (i) a proton conduction between two neighboring $OH^- \ldots OH^-$ ions ($OH^- + OH^- \rightarrow O^{2-} + HOH$) and (ii) a proton jump from the first OH^- ion to the next via the PO_4^{3-} ions. We then propose the mechanism

$$2OH^- + [PO_4]^{3-} \rightarrow O^{2-} + [HPO_4]^{2-} + OH$$
$$\rightarrow O^{2-} + [PO_4]^{3-}\ HOH + \square_{OH^-},$$

where ($\square_{OH^-}$) indicates a vacancy at an OH^- lattice site, while O^{2-} is an oxide ion converted from an OH^- ion. The last mechanism has been observed during the formation of dental caries by protonation process of PO_4^{3-} ions contained in the tooth. Therefore, proton transport along an OH^- chain in an apatite is probably the elementary step in

TABLE 3
Comparison of Electrical Properties between Fluoroapatite and Hydroxyapatite Materials in Relation with Physical Characteristics of M^{2+} Ions

	M^{2+} ions		
	Ca^{2+}	Ba^{2+}	Pb^{2+}
Fluorapatites			
log σ_{800} (S/cm)	− 4.452	− 3.890	− 3.563
Activation energy E_a (eV)	1.86	1.47	0.25 1.36
Hydroxyapatites			
log σ_{800} (S/cm)	− 6.127	− 5.740	− 4.637
Activation energy E_a (eV)	1.21	1.27	0.62 1.60
Ionic radius of M^{2+} ion [Å] (14)	0.99	1.34	1.20
Polarizability of M^{2+}ion 10^{-24}[cm^{-1}] (13)	0.60	1.60	3.60

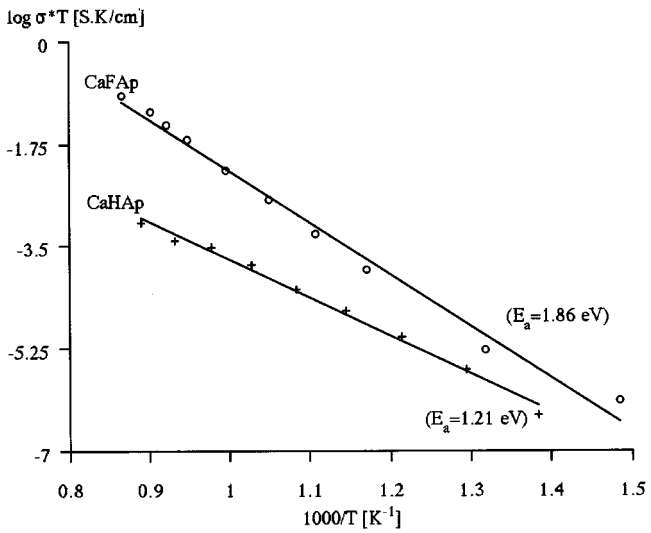

FIG. 3. Comparison of electrical properties between calcium fluoroapatite and calcium hydroxyapatite samples.

the acid attack, which initiates demineralization and eventually leads to caries lesions (2, 17, 18). Based on structural results, the distance between two adjacent OH^- ions is 3.44 Å ($M = Ca$), too large for protons to hop (16). However, the distance between an OH^- and its adjacent PO_4^{3-} is 3.07 Å, short enough to form an hydrogen bond between the hydrogen-containing OH^- ions and the double-bonded oxygen of PO_4^{3-} ions. This can best be described by the choice of the second mechanism in stoichiometric apatites.

At high temperature, the proton hopping can move along the c axis between the electroactive O^{2-} anions converted from OH^- ions after dehydration of hydroxyapatite according to the reaction

$$Ca_{10}(PO_4)_6(OH)_2 \rightarrow Ca_{10}(PO_4)_6(OH)_{2-2x}O_x\square_x + H_2O.$$

The same conduction has been observed in the yttrium-substituted calcium oxyhydroxyapatite $Ca_{10-x}Y_x(PO_4)_6(OH)_{2-x}O_x\square_x$, considering that O^{2-} ions are the electroactive species for proton conduction (19). However, in lanthanum-substituted calcium vanadates $Ca_{10-x}La_x(VO_4)_6O_{1+x/2}\square_{1-x/2}$ $(0 \leq x \leq 2)$, the O^{2-} ions are considered the main charge carrier (20). It was found in terms of electrical conductivity that the conduction mechanism depends on the apatite composition. Therefore, the nonstoichiometry of hydroxyapatite can influence the proton conduction (21).

4. CONCLUSION

The electrical conductivity of apatite materials is related mainly to their composition and to the physical chemistry parameters such as ionic radius and polarizability. Comparing the ionic conductivity results of fluoroapatite and hydroxyapatite electrolytes, we note that the lead apatite presents some differences as a function of the temperature, which are related to Pb–X bond. On the other hand, the fluoroapatite is a better conductor than hydroxyapatite materials. This is in relation to the nature of the hopping species.

ACKNOWLEDGMENT

We express our thanks to Professor Jacques Livage (Paris) for valuable scientific discussions.

REFERENCES

1. L. Hench, *J. Am. Ceram. Soc.* **74,** 1487 (1991).
2. J. C. Elliot, "Studies in Inorganic Chemistry," Vol. 18, Elsevier, Amsterdam, 1994.
3. J. O. Nriagu and P. B. Moore, "Phosphate Minerals," p. 9. Springer-Verlag, Berlin, 1984.
4. M. Chusmans, C. Longbottom, P. Los, and P. G. Bruce, *J. Dent. Res.* **75,** 1871 (1996).
5. R. Z. Legros, "Monographs in Oral Science" (H. M. Meyers, Eds.), Vol. 15. San Francisco, 1991.
6. Y. Konime and K. Sato, *Fine Ceram. Rep.* **1,** 4 (1983).
7. H. Monma, *J. Catal.* **75,** 20 (1982).
8. A. Laghzizil, A. Bouhaouss, S. El Hajjaji, and M. Ferhat, *Solid State Ionics* **126,** 245 (1999).
9. A. Laghzizil, A. Bouhaouss, and M. Ferhat, *Phos. Res. Bull.* **10,** 381 (1999).
10. A. Laghzizil, P. Barboux, and A. Bouhaouss, *Solid State Ionics* **128,** 177 (2000).
11. M. Andres-Verges, F. J. Higes-Rolando, and P.F. Gonzalez-Dias, *J. Solid State Chem.* **43,** 237 (1982).
12. M. Andres-Verges, F. J. Higes-Rolando, C. Valenzuela-Calahorro, P. F. Gonzalez-Dias, *Spectrochim. Acta* **39,** 1077 (1983).
13. M. Garric, "Cours de Chimie." Dunod, Paris, 1976.
14. E. E. Dreenwood, "Ionic Crystals Lattice, Defects and Nonstoichiometry." Butterworths London, 1968.
15. A. Laghzizil, "Etude de la conductivité des Fluorapatites; Correlation entre les proprietés electriques et structurales," thesis. Université Mohamed V, Rabat, 1993.
16. K. Yamashita, K. Kitagaki, and T. Umegaki, *J. Am. Ceram. Soc.* **78,** 1191 (1995).
17. H. L. Margolis and E. C. Morero, *Caries Res.* **11,** 22 (1989).
18. P. Anderson and J. C. Elliot, *J. Dent. Res.* **71,** 1473 (1992).
19. K. Yamashita, H. Owada, T. Umegaki, T. Kanazawa, and T. Futagami, *Solid State Ionics* **28–30,** 660 (1990).
20. H. Bemoussa, M. Mikou, A. Benssaoud, A. Bouhaouss, and R. Morineau, *Mater. Res. Bull.* **34,** 1439 (2000).
21. K. Yamashita, K. Kitagaki, T. Umegaki, and T. Kanazawa, *J. Mat. Sci. Lett.* **9,** 4 (1990).